Publication V

R. C. D. Paiva, J. Pakarinen, and V. Välimäki. Reduced-complexity modeling of high-order nonlinear audio systems using swept-sine and principal component analysis. In *Proc. AES 45th Conf. Applications of Time-Frequency Processing in Audio*, Espoo, Finland, pp. 1–4, Mar. 2012.

Reduced-complexity modeling of high-order nonlinear audio systems using swept-sine and principal component analysis

Rafael Cauduro Dias de Paiva[1,2], Jyri Pakarinen[1] and Vesa Välimäki[1]

[1]*Aalto University School of Electrical Engineering, Department of Signal Processing and Acoustics, Espoo, Finland*

[2]*Nokia Technology Institute INdT, Brasilia, Brazil*

Correspondence should be addressed to Rafael Cauduro Dias de Paiva (rafael.dias.de.paiva@aalto.fi)

ABSTRACT

Modeling high-order nonlinear systems is an important issue in audio signal processing. It may be employed in real-time emulation of analog nonlinear systems, such as guitar distortion and amplifiers or other vintage electronic audio systems. This paper proposes a new method for obtaining an economical black-box model of nonlinear systems using the swept-sine technique, which extracts the harmonic distortion at each frequency by separating them in time. In the proposed model the swept-sine technique is used to obtain the time-frequency representation of a nonlinear system, and the principal component analysis is used to reduce the complexity of the model. It is shown that the proposed method reduces the computational cost by 66% when compared to traditional swept-sine models.

1. INTRODUCTION

Nonlinear analog audio systems have an important contribution to the timbre of musical instruments. This is the case for the amplifiers and effect boxes used with guitars, as well as for the circuits used in analog synthesizers. For that reason, many musicians would benefit from computer simulation of this type of system. However, this is not a trivial task, and it is a common belief that musicians often prefer the original analog products due to their sound quality. The objective of this paper is to provide an efficient black-box method for modeling high-order nonlinear systems.

Modeling of nonlinear audio systems follows one of two basic approaches. The first one consists of physical models [1, 2]. In this approach the physical phenomena involved in the nonlinear system is described and used to obtain a digital counterpart of an audio system. Examples of this type of approach include solving ordinary differential equations of the system [3, 4], state-space models [5, 6], the K-method [7, 8], behavioral models [9] and wave digital filters [10, 11, 12, 13]. This type of modeling approach provides an excellent way for obtaining accurate models whose parameters can usually be modified in a simplified manner. However, physical modeling requires a detailed knowledge of the system being modeled, which will not always be possible in practice.

The second approach for modeling nonlinear audio systems is a black-box approach. In this approach no physical knowledge of the system is required, and a model that emulates the same input/output relationship is obtained. This approach includes Volterra models [14], which are capable of representing any kind of nonlinear system with memory. However, the kind of nonlinear systems generally used in analog audio processing often have large orders, which would yield very complex Volterra filters. Some simplifications on the Volterra filters can be obtained using the Wiener or Hammerstein models, in which a static nonlinear function is used in series with a linear filter [15]. However, there are no good methods available for identification of this type of system suitable for this kind of simplification in an automatic manner.

Other black-box methods emerge from the use of swept-sine analysis methods. The swept-sine method was originally used for the analysis of the harmonic components that are generated by nonlinear systems [16]. The swept-sine was then further extended for obtaining a black-box model of nonlinear systems consisting of several poly-

nomial Hammerstein models in parallel [17, 18, 19]. Although this method provides a simplified approach for obtaining a nonlinear model of audio systems, it would be prohibitively expensive when high-order nonlinearities are used, which is often the case of guitar distortion circuits.

This work presents a new solution for modeling high-order audio nonlinearities using a black-box approach. In the proposed method, the swept-sine analysis is used to obtain the frequency response of each harmonic of the nonlinear system [16]. As a second step, the proposed method improves the swept-sine analysis by simplifying its result through the use of the principal component analysis (PCA) method. PCA is traditionally used for information compression [20]. Hence, the combination of PCA and the swept-sine analysis yields a black-box model with lower computational complexity. The great advantage of this method is that high-order nonlinear systems can be represented with a small number of components, whereas traditional swept-sine approaches would need the same number of components as the order of the system. The results shown in this paper prove that systems of order 30 can be represented with three to eight components, while other swept-sine methods require 30 components.

This paper is organized as follows. Sec. 2 presents a review on the swept-sine method. Sec. 3 presents the improvement over the swept-sine method using PCA. Sec. 4 describes the system under measurement and the method for measuring its response. Sec. 5 shows the modeling results, and the advantages of the proposed method. Sec. 6 presents the interpretation of the results and discussion on the compromise between the accuracy and the computational complexity of the model. Sec. 7 concludes the paper.

2. NONLINEAR SYSTEM IDENTIFICATION WITH SWEPT-SINE

The swept-sine technique is used for determining the nonlinear response of a system [17]. With this technique, it is possible to analyze the nonlinear response of a system, or to obtain a black-box model of the analyzed system, such as in Fig. 1.

In this method, one chirp signal excites the system while the response to this signal is measured at the output. The swept-sine excitation is obtained as [17, 18]

$$x_e(n) = \sin\left[2\pi T\left(e^{\frac{f_1 n}{T f_s}} - 1\right)\right] \tag{1}$$

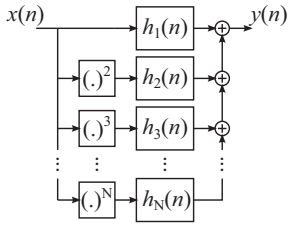

Figure 1: Generalized polynomial Hammerstein model (adapted from [18]).

where T is the total length of the signal $x_e(n)$, f_s is the sampling frequency, and f_1 is the initial frequency of the swept-sine.

The total length of the signal T needs to be determined in order to obtain phase coherency between the harmonic responses obtained with this method. A known property of the swept-sine signal is that the phase difference between points of $x_e(n)$ with integer multiple instantaneous frequency is constant. For that reason, T is chosen such that the phase shift for the k^{th} harmonic is $2\pi M$, or, equivalently [19]

$$T = \left(\frac{2\pi M}{k-1} - \frac{\pi}{2}\right)\frac{\ln f_2/f_1}{2\pi f_1}, \tag{2}$$

where f_2 is the final frequency of the sweep. In this work, it was observed that it is sufficient to guarantee the phase shift for the second harmonic, hence $k = 2$ and M is chosen to approximate the desired swept-sine length in seconds.

Once the excitation signal $x_e(n)$ is calculated as in Eq. 1, this signal is fed into the system under test. The response to $x_e(n)$ is measured at the output of the system $y_e(n)$, which is then inverse filtered [19] by

$$X_i(f) = \frac{X_e^*(f)}{|X_e(f)|^2 + \varepsilon(f)}, \tag{3}$$

where $X_i(f) = \mathscr{F}(x_i(n))$ is the frequency response of the inverse filter, $\varepsilon(f)$ is a function used for regularization of the inverse of the excitation signal $X_e(f) = \mathscr{F}(x_e(n))$ outside the band $f_1 < f < f_2$. The resulting signal $y_i(n) = y_e(n) * x_i(n)$ contains the composition of the impulse responses $g_k(n)$ of the k^{th} harmonics, which are shifted by

$$\Delta n_k = \frac{T f_s \ln k}{\ln(f_2/f_1)} \tag{4}$$

samples. Notice that the values Δn_k will have fractional sample times. Thus, the impulse responses $g_k(n)$ are obtained by windowing the $y_i(n)$ at the time instants Δn_k. Finally, the impulse responses $h_k(n)$ for each k$^{\text{th}}$ polynomial nonlinearity, are obtained using Chebyshev polynomials [18, 19].

3. IMPROVED SWEPT-SINE USING PRINCIPAL COMPONENT ANALYSIS

The swept-sine method provides a good automatic way of obtaining a black-box model of a nonlinear system. However, when high-order nonlinear systems are used, the decomposition of Fig. 1 yields a very complex model. Hence, for a nonlinear system with order N, it is desirable to obtain a simplified computational model in which M waveshaper/filter pairs are used, with $M < N$, as in Fig. 2. A possible solution for that problem is achieved through the use of principal component analysis (PCA).

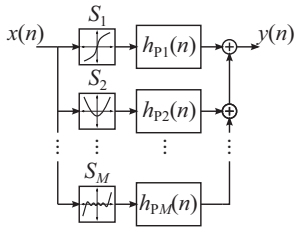

Figure 2: Simplified Hammerstein model using principal component analysis.

Once the impulse responses of each harmonic $g_k(n)$ are obtained as in Section 2, they are grouped in a matrix $\mathbf{G}$ as

$$\mathbf{G} = \begin{bmatrix} g_1(0) & g_1(1) & \dots & g_1(L) \\ g_2(0) & g_2(1) & \dots & g_2(L) \\ \vdots & \vdots & \ddots & \vdots \\ g_N(0) & g_N(1) & \dots & g_N(L) \end{bmatrix}, \tag{5}$$

where L is the maximum length of the impulse responses $g_k(n)$.

In a second step, a matrix $\mathbf{C}$ with an estimative of the covariance between the impulse responses $c_{k,l} = \mathrm{E}[(g_k - \bar{g_k})(g_l - \bar{g_l})]$ is obtained as

$$\mathbf{C} = \left(\mathbf{G} - \bar{\mathbf{G}}\right)\left(\mathbf{G} - \bar{\mathbf{G}}\right)^{\mathrm{T}} \tag{6}$$

$$= \begin{bmatrix} c_{1,1} & c_{1,2} & \dots & c_{1,N} \\ c_{2,1} & c_{2,2} & \dots & c_{2,N} \\ \vdots & \vdots & \ddots & \vdots \\ c_{N,1} & c_{N,2} & \dots & c_{N,N} \end{bmatrix},$$

where the superscript T denotes matrix transposition, and $\bar{\mathbf{G}}$ is a $N \times L$ matrix with the averages of $g_k(n)$. If the eigendecomposition is applied to the covariance matrix $\mathbf{C}$, we obtain

$$\mathbf{C} = \mathbf{Q}\mathbf{A}\mathbf{Q}^T, \tag{7}$$

where $\mathbf{Q}$ is an orthogonal matrix with the eigenvectors $\mathbf{q}_k$ of $\mathbf{C}$ in its k columns,

$$\mathbf{q}_k = \begin{bmatrix} q_k(1) & q_k(2) & \dots & q_k(N) \end{bmatrix}^{\mathrm{T}} \tag{8}$$

and $\mathbf{A}$ is a diagonal matrix with eigenvalues a_k corresponding to each eigenvector $\mathbf{q}_k$.

Each eigenvector $\mathbf{q}_k$ can be understood as one principal direction in which the data on $\mathbf{G}$ varies. This can be used for mapping $\mathbf{G}$ into this direction as

$$\begin{aligned} \mathbf{h}_{\mathrm{P}k} &= \mathbf{q}_k^{\mathrm{T}}\mathbf{G} \\ &= \begin{bmatrix} h_{\mathrm{P}k}(0) & h_{\mathrm{P}k}(1) & \dots & h_{\mathrm{P}k}(L) \end{bmatrix}, \end{aligned} \tag{9}$$

where the energy of $\mathbf{h}_{\mathrm{P}k}$ is given by the eigenvalue a_k. Hence, since the eigenvectors are normalized, the eigenvectors with larger eigenvalues represent the principal directions of $\mathbf{G}$ [20]. This result can be used to compress the information contained in $\mathbf{G}$, by using only the main M impulse responses $h_{\mathrm{P}k}(n)$ with large a_k to represent a nonlinear system as in Fig. 5, or equivalently

$$y(n) = \sum_{k=0}^{M} S_k\left(x(n)\right) * h_{\mathrm{P}k}(n), \tag{10}$$

where $S_k(x)$ is a waveshaper responsible for generating the harmonics in the eigenvector $\mathbf{q}_k$, and $*$ denotes convolution. The shape of $S_k(x)$ is calculated as

$$S_k(x) = \sum_{l=0}^{N-1} q_l(k) T_l(x), \tag{11}$$

where $T_k(x)$ is the Chebyshev polynomial of order k with x as input argument.

In practice, the energy of each harmonic response $g_k(n)$ decays as the order k increases. For that reason, if the principal components decomposition is directly applied

on the matrix $\mathbf{G}$, the resulting principal components will be biased for modeling only the harmonic components with more energy. In order to mitigate this problem, it is possible to normalize the energy of the responses $g_k(n)$. However, low-energy responses $g_k(n)$ may be corrupted by noise and may not be perceptually important for the final model. This may be the case of even harmonics in some distortion circuits. Hence, an alternative solution was developed. Firstly, the energy of each harmonic component in dB is calculated

$$E_k = 10\log_{10}\left(\frac{1}{L}\sum_{l=0}^{L}|g_k(l)|^2\right). \quad (12)$$

The envelope energy decay is approximated with a third order polynomial $p(k)$. This is done in order to avoid increasing the energy of low energy harmonics close to high energy harmonics, i.e. harmonics with $E_{k-1} \gg E_k \ll E_{k+1}$. Finally, each impulse response is multiplied by an energy dependent factor, yielding the normalized impulse responses as

$$\tilde{g_k}(n) = g_k(n)10^{\frac{p(k)}{10\gamma}}, \quad (13)$$

where γ is the normalization factor. In the example shown in Section 5 the practical value of the normalization factor was $\gamma = 4$. Hence, a normalized impulse responses matrix is obtained as $\tilde{\mathbf{G}}$, which is used to obtain the normalized correlation matrix $\tilde{\mathbf{C}}$ and its corresponding normalized eigenvector $\tilde{\mathbf{Q}}$ and eigenvalue $\tilde{\mathbf{A}}$ matrices, with eigenvectors $\tilde{\mathbf{q}}_k$ and eigenvalues $\tilde{a}_k$.

Additionally, another useful simplification of the method can be obtained by ignoring low energy elements of the correlation matrix $\mathbf{C}$ or $\tilde{\mathbf{C}}$. This approach is particularly interesting in systems that have low energy at even or odd harmonics. In that case, even and odd harmonics are artificially decorrelated by changing the correlation matrix $\mathbf{C}$ as

$$C_{\text{eo}}(k,l) = \begin{cases} C(k,l), & \text{if } k+l \text{ is even,} \\ 0, & \text{otherwise} \end{cases}. \quad (14)$$

If normalization is used, the normalized correlation matrix $\tilde{\mathbf{C}}$ can be modified as

$$\tilde{C}_{\text{eo}}(k,l) = \begin{cases} \tilde{C}(k,l), & \text{if } k+l \text{ is even,} \\ 0, & \text{otherwise} \end{cases}. \quad (15)$$

Some practical aspects need to be considered when applying this method. In order for the PCA method to be able to consistently detect the correlation between the impulse responses $g_k(n)$, it is important that they are perfectly synchronized in $\mathbf{G}$. For that purpose, the fractional center of the impulse response Δn_k in Eq. 4 needs to be compensated using a fractional delay filter [21]. As the analysis phase is performed off-line, the computational complexity was not considered important for the analysis. Hence, a 91-samples long windowed sinc function was used as the fractional delay filter. Additionally, the phase-shift between the harmonic responses $g_k(n)$ needs to be guaranteed using swept-sine excitation length as in Eq. 2. If any of these aspects are ignored, the PCA method will fail, and the principal components obtained will contain most of their energy on a single harmonic component. In that case, no complexity reduction is achieved.

4. MEASUREMENT SETUP

Measurements of a practical distortion circuit were performed in order to demonstrate the behavior of the proposed modeling approach. A Tube Screamer TS9 distortion circuit was measured as in Fig. 3. For that purpose, an excitation signal $x_e(n)$ was used as the input of the system, while the response of the system $y_e(n)$ was measured at the output. The excitation signal $x_e(n)$ consisted of a swept-sine signal calculated as in Eq. 1, with minimum frequency $f_1 = 10$ Hz, maximum frequency $f_2 = 20$ kHz, sampling frequency $f_s = 48$ kHz, and length of $T = 10.4512$ s. The input signal was generated using a computer connected to the distortion circuit under test through its sound-card output. The output of the system was obtained using the microphone input of the sound-card. The distortion effect parameters were kept constant during the measurement, with the volume, distortion and tone controls at their maximum levels.

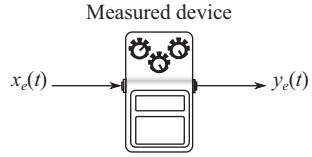

Figure 3: Measurement setup.

5. RESULTS

This section presents the measurement results obtained for a Tube Screamer TS9 distortion circuit, and compares

it to the results obtained with the proposed model. In this section, the normalized harmonic impulse response matrix $\tilde{\mathbf{G}}$ is obtained using the swept-sine method with normalization factor $\gamma = 4$, and truncated so that it has 99.97% of the energy. The swept-sine response was oversampled at 96 kHz. This yielded finite impulse response (FIR) filters with 1435 coefficients. Additionally, since even harmonics have low energy in this system, the correlation between even and odd harmonics was ignored, as in Eq. 15. Fig. 4 shows the time-frequency representation of the excitation signal and the measured output signal, in Fig. 4 (a) and (b) respectively.

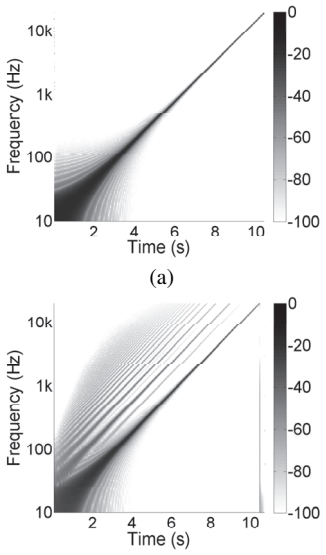

Figure 4: Spectrogram of the (a) swept-sine excitation signal and (b) the measured output signal in dB. Spectrogram generated using 300 logarithmically spaced frequencies between 10 Hz and 20 kHz, 4800 samples long Hanning window with 50% overlap.

The magnitude of the main six principal components $\tilde{\mathbf{q}}_k$ is represented in Fig. 5. In Fig. 5 it is possible to observe that each principal component is responsible for representing a different set of harmonic components. The first component has energy concentration mainly at the fundamental frequency, with attenuated energy at the third, fifth and seventh harmonic components, while the other principal components have increased energy for higher order harmonic components. Additionally, it is possible to observe that none of the represented principal components $\tilde{\mathbf{q}}_k$ represents the even harmonics. This indicates that the generation of even harmonics is not as important as that of the odd harmonics in this particular circuit.

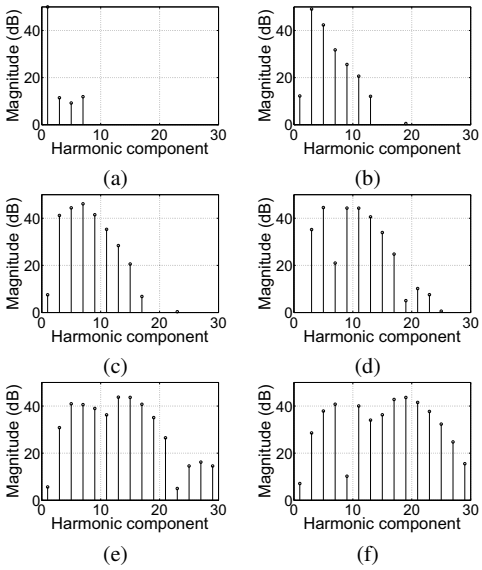

Figure 5: Magnitude of each harmonic component obtained for the distortion circuit under analysis with PCA for the (a) first, (b) second, (c) third, (d) fourth, (e) fifth and (f) sixth components.

The resulting nonlinear shapes obtained with PCA are represented in Fig. 6. The shapes are obtained by using the Chebyshev polynomials for mapping the principal components $\tilde{\mathbf{q}}_k$ into nonlinear functions $S_k(x)$, as in Eq. 11. The first principal component waveshaper $S_1(x)$ in Fig. 6 (a) is a smooth nonlinearity with odd symmetry, which is in line to the harmonic content observed in Fig. 5 (a). The other waveshapers have increased complexity as the principal component number increases, in Fig. 6 (b-f) for the second to the sixth components. This result is also in line with the results in Fig. 5 (b-f), where higher order harmonics are mostly observed in the fourth to the sixth principal components.

In addition to the waveshapers, each principal component of the nonlinear system has a corresponding filter

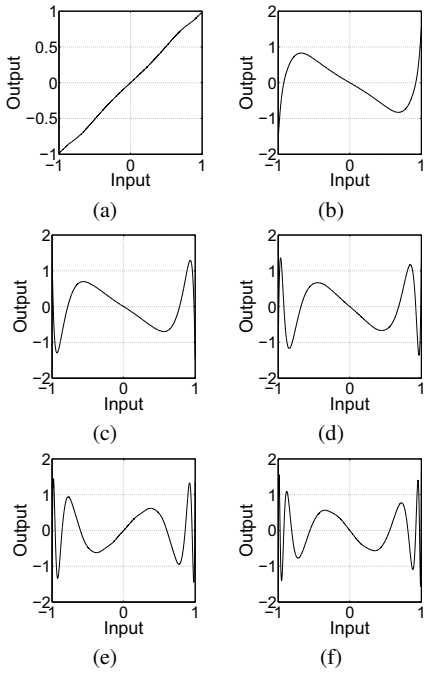

Figure 6: Nonlinear functions $S_k(x)$ obtained for the distortion circuit under analysis with PCA for the (a) first, (b) second, (c) third, (d) fourth, (e) fifth and (f) sixth components.

$h_{Pk}(n)$, as indicated in Fig. 2. The impulse response of this filter is obtained using $\tilde{\mathbf{q}}_k$ and $\mathbf{G}$ as in Eq. 9. The magnitude of the frequency response for the corresponding filter of the first six principal components is presented in Fig. 7. It is possible to observe that the magnitude of the first principal component $h_{P1}(n)$ is larger than for the others. Additionally, the frequency response of each component presents a different frequency pattern. The combination of the nonlinear functions in Fig. 6 with the filters in Fig. 7 completes the nonlinear model of Fig. 2.

The result of the combination of the waveshapers and filters is presented in Fig. 8. In this figure, the response of a single principal component is illustrated, where the swept-sine signal of Fig. 4 (a) excites a nonlinear model with a waveshaper $S_k(x)$, and a filter $h_{Pk}(n)$. This time-frequency representation shows that each principal component is responsible for modeling a group of harmonics.

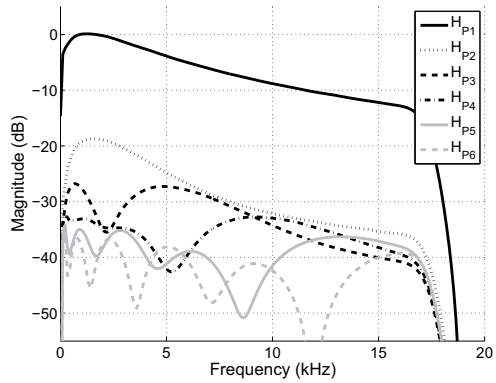

Figure 7: Frequency response of the first six principal components.

Additionally, it is also possible to observe that the energy of the responses is larger for the first principal components. Some aliasing can be observed in Fig. 8, which is handled in practice by oversampling.

One indication of how many principal components are needed for representing this nonlinear system is given in Fig. 9. In this figure, the percentage of energy that is represented with a number of principal components is given. Two energy measures are presented in this figure. The first one is the normalized energy, which is obtained with the cumulative sum of the eigenvalues $\tilde{a}_k$ of the normalized correlation matrix $\tilde{\mathbf{C}}$. The second one is obtained with the absolute value of the represented energy when using the first M eigenvectors $\tilde{\mathbf{q}}_k$, for $k = 1 \ldots M$. In both cases 99% of the energy is represented with two to eight components, which indicates that it is possible to reduce the complexity of the nonlinear model using PCA.

The comparison results of the measured nonlinear system (called *Ref.* in the results), and the models with three, five and eight principal components are shown in Fig. 10. The results show the swept-sine analysis for the odd harmonics, up to the 27th harmonic. The results for the even harmonics are omitted, due to their lower energy in comparison to the odd ones. When using three principal components the modeled nonlinear system is able to represent the reference nonlinear system up to the ninth harmonic for excitation signals with fundamental frequency bellow 1.5 kHz. When five principal components are used, 13 to 15 harmonics are represented

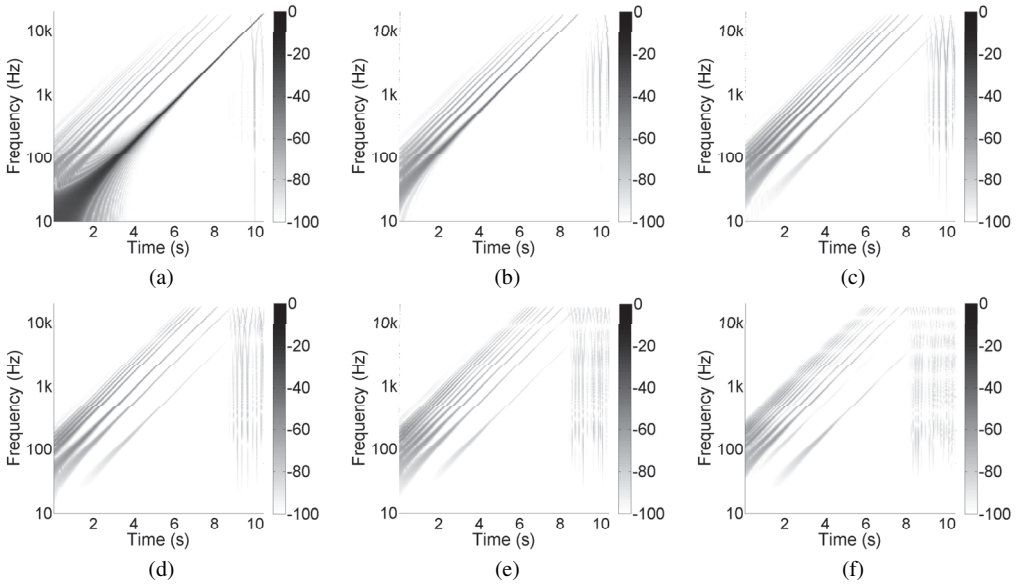

Figure 8: Spectrogram of the PCA waveshaper/filter pairs obtained with a swept-sine input of 10.4512 s for the distortion circuit under analysis for the (a) first, (b) second, (c) third, (d) fourth, (e) fifth and (f) sixth components in dB.

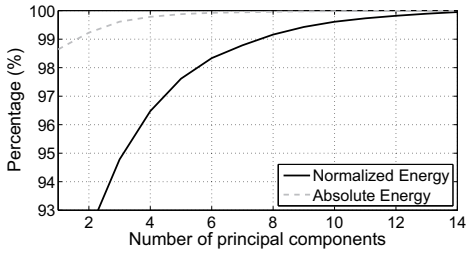

Figure 9: Percentage of the energy represented when using different number of principal components.

with some oscillation at low frequencies. When using eight principal components, the model is able to represent the nonlinear system up to the 27th harmonic. However, some random oscillation is observed for high order harmonics.

6. COMPARISON AND DISCUSSION

In all the presented examples, the proposed method provides a less expensive model when compared to the model obtained with the swept-sine method without PCA. In order to represent nine harmonics, the swept-sine method requires nine nonlinear functions followed by nine filters. When using PCA, the proposed system reduces 66% of the computational cost, since it uses three principal components. Moreover, when using five and eight principal components, the resulting nonlinear system reduces 66% of the computational cost for representing 15 and 27 harmonics, respectively. Hence, with the proposed model it is possible to obtain high-order nonlinear systems with reduced computational complexity.

The balance between the number of represented harmonics and how accurate the resulting system will be is controlled when selecting the number of principal components, and the normalization factor γ in Eq. 13. With a small normalization factor, i.e. $\gamma = 1$, the energy envelope of the harmonics is compensated and the higher harmonics will have the same weight as the lower ones. However, the estimation of the impulse responses for the higher order harmonics is not as accurate as for the lower

ones, making the system more susceptible to noise, and leading to numerical problems when obtaining $\tilde{\mathbf{Q}}$.

On the other hand, the larger the number of principal components, the more accurate will be the impulse response of each harmonic component $g_k(n)$. This leads to a compromise between the desired modeling accuracy and the available computation capacity for running the model.

Finally, the application of PCA can simplify model interpolation when representing different parameter sets of the modeled system. In order to represent different parameters of a nonlinear analog system, the swept-sine model has to be derived considering different values for these parameters. Since all possible values cannot be measured, interpolation between the models corresponding to different parameter sets is necessary. When PCA is applied, the number of impulse responses that need to be interpolated is reduced. This can greatly reduce the number of operations required when changing parameters of the original analog system.

7. CONCLUSIONS

This paper has presented a solution for obtaining a black-box model of high-order nonlinear system using the swept-sine method. In the proposed approach the swept-sine method is used for estimating the frequency responses of each harmonic generated by the nonlinear system, and the principal component analysis (PCA) is used to derive a low order model that represents this system. The PCA is used to obtain the similarities between the impulse responses of each harmonic component, yielding nonlinear functions and filters that represent each of these components.

The proposed method has shown that it is possible to reduce by 66% the computational cost required for modeling high-order nonlinear systems. This results in a system that is better suited for real-time implementation in plugins and applications emulating high-order distortion circuits than the original system.

This method may be used not only for models of nonlinear systems, but also for obtaining compact representations for analyzing these systems. The swept-sine analysis has been used also for comparing the frequency response of nonlinear systems. However, this analysis is practical only for a limited number of harmonics. Hence, after obtaining the principal components of that system, the frequency response of some principal components can be analyzed individually instead of the frequency response for a large number of harmonics.

ACKNOWLEDGEMENTS

The authors are grateful to Julian Parker for his comments on the manuscript. This research was funded by Academy of Finland (Project 122815).

8. REFERENCES

[1] V. Välimäki, J. Pakarinen, C. Erkut, and M. Karjalainen, "Discrete-time modelling of musical instruments," *Reports on Progress in Physics*, vol. 69, no. 1, pp. 1–78, January 2006.

[2] J. Pakarinen and D. T. Yeh, "A review of digital techniques for modeling vacuum-tube guitar amplifiers," *Computer Music Journal*, vol. 33, no. 2, pp. 85–100, 2009.

[3] D. T. Yeh, J. S. Abel, A.Vladimirescu, and J. O. Smith, "Numerical methods for simulation of guitar distortion circuits," *Computer Music Journal*, vol. 32, no. 2, pp. 23–42, 2008.

[4] J. Macak and J. Schimmel, "Real-time guitar tube amplifier simulation using an approximation of differential equations," in *Proc. of the DAFx'10, 13th International Conference on Digital Audio Effects*, Graz, Austria, September 2010.

[5] K. Dempwolf, M. Holters, and U. Zölzer, "Discretization of parametric analog circuits for real-time simulations," in *Proc. of the DAFx'10, 13th International Conference on Digital Audio Effects*, Graz, Austria, September 2010, pp. 1–8.

[6] I. Cohen and T. Hélie, "Real-time simulation of a guitar power amplifier," in *Proc. of the DAFx'10, 13th International Conference on Digital Audio Effects*, Graz, Austria, September 2010.

[7] D. Yeh, J. Abel, and J. Smith, "Automated physical modeling of nonlinear audio circuits for real-time audio effects – part I: Theoretical development," *IEEE Transactions on Audio, Speech, and Language Processing*, vol. 18, no. 4, pp. 728–737, May 2010.

[8] G. Borin, G. De Poli, and D. Rocchesso, "Elimination of delay-free loops in discrete-time models

of nonlinear acoustic systems," *IEEE Transactions on Speech and Audio Processing*, vol. 8, no. 5, pp. 597–605, September 2000.

[9] J. Parker, "A simple digital model of the diode-based ring-modulator," in *Proc. of the DAFx'11, 14th International Conference on Digital Audio Effects*, Paris, France, September 2011.

[10] A. Sarti and G. De Sanctis, "Systematic methods for the implementation of nonlinear wave-digital structures," *IEEE Transactions on Circuits and Systems I: Regular Papers*, vol. 56, no. 2, pp. 460–472, February 2009.

[11] J. Pakarinen and M. Karjalainen, "Enhanced wave digital triode model for real-time tube amplifier emulation," *IEEE Transactions on Audio, Speech, and Language Processing*, vol. 18, no. 4, pp. 738–746, 2010.

[12] R. C. D. Paiva, J. Pakarinen, V. Välimäki, and M. Tikander, "Real-time audio transformer emulation for virtual tube amplifiers," *EURASIP Journal on Advances in Signal Processing*, vol. 2011, pp. 1–15, 2011.

[13] A. Fettweis, "Wave digital filters: Theory and practice," *Proc. of the IEEE*, vol. 74, no. 2, pp. 270–327, February 1986.

[14] T. Hélie, "Volterra series and state transformation for real-time simulations of audio circuits including saturations: Application to the Moog ladder filter," *IEEE Transactions on Audio, Speech, and Language Processing*, vol. 18, no. 4, pp. 747–759, May 2010.

[15] T. Ogunfunmi, *Adaptive Nonlinear System Identification: The Volterra and Wiener Model Approaches*. Springer Series in Signals and Communication Technology, 2007.

[16] A. Farina, "Simultaneous measurement of impulse response and distortion with a swept-sine technique," in *108th Audio Engineering Society Convention*, Paris, France, February 2000, preprint 5093.

[17] ——, "Non-linear convolution: A new approach for the auralization of distorting systems," in *110th Audio Engineering Society Convention*, Amsterdam, The Netherlands, May 2001, preprint 5359.

[18] A. Novák, L. Simon, and P. Lotton, "Analysis, synthesis, and classification of nonlinear systems using synchronized swept-sine method for audio effects," *EURASIP Journal on Advances in Signal Processing*, vol. 2010, p. 8, 2010.

[19] M. Rébillat, R. Hennequin, E. Corteel, and B. F. Katz, "Identification of cascade of Hammerstein models for the description of nonlinearities in vibrating devices," *Journal of Sound and Vibration*, vol. 330, no. 5, pp. 1018–1038, February 2011.

[20] I. T. Jolliffe, *Principal Component Analysis*, 2nd ed. Springer Series in Statistics, 2002.

[21] T. I. Laakso, V. Välimäki, M. Karjalainen, and U. K. Laine, "Splitting the unit delay - tools for fractional delay filter design," *IEEE Signal Processing Magazine*, vol. 13, no. 1, pp. 30 – 60, January 1996.

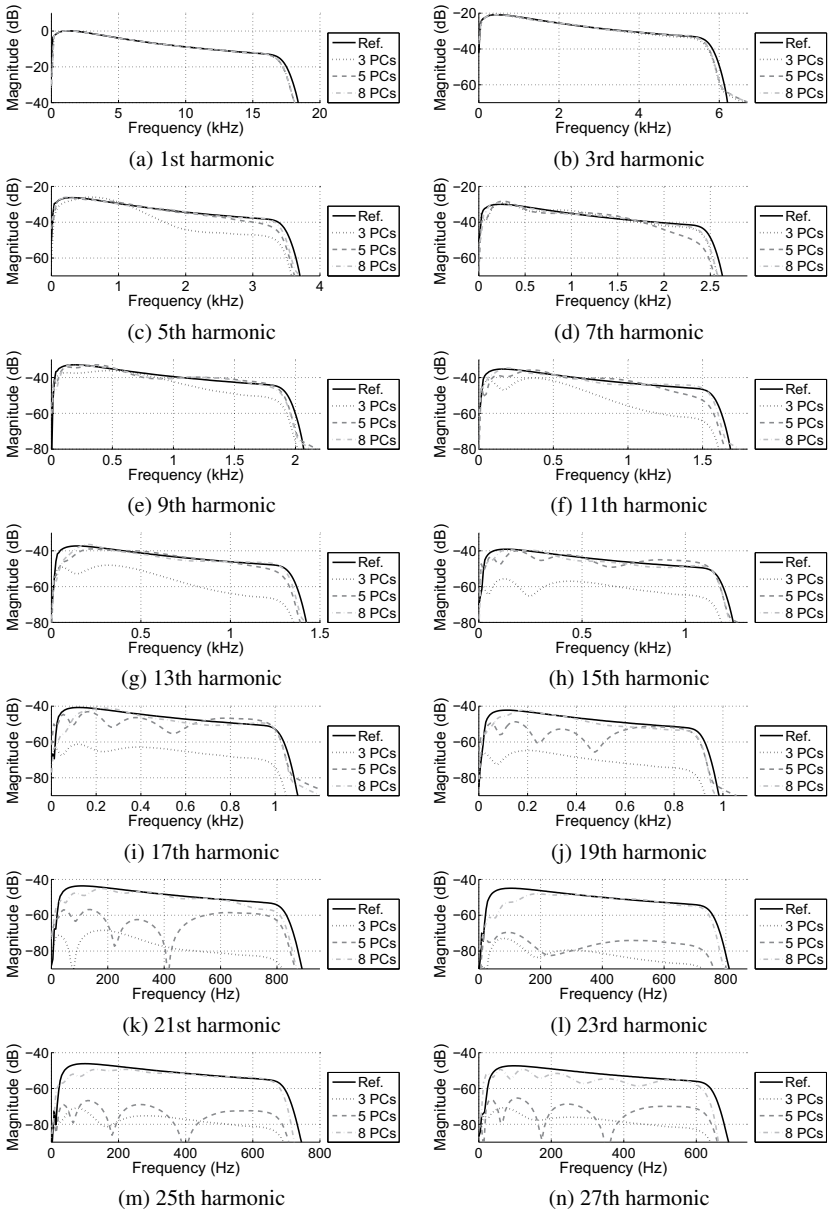

(a) 1st harmonic (b) 3rd harmonic

(c) 5th harmonic (d) 7th harmonic

(e) 9th harmonic (f) 11th harmonic

(g) 13th harmonic (h) 15th harmonic

(i) 17th harmonic (j) 19th harmonic

(k) 21st harmonic (l) 23rd harmonic

(m) 25th harmonic (n) 27th harmonic

Figure 10: Swept-sine analysis results of the distortion circuit (Ref.) and the modeled versions of the circuit with three, five and eight principal components.